# Recent results in Jülich solid oxide fuel cell technology development

Ludger Blum [a,*], L.G.J. (Bert) de Haart [a], Jürgen Malzbender [a], Norbert H. Menzler [a], Josef Remmel [a], Robert Steinberger-Wilckens [b]

[a] Forschungszentrum Jülich GmbH, Wilhelm-Johnen-Straße, D-52428 Jülich, Germany
[b] School of Chemical Engineering, College of Engineering and Physical Sciences, University of Birmingham, Edgbaston B15 2TT, UK

## HIGHLIGHTS

- Development status at Forschungszentrum Jülich concerning cells, stack and system.
- Optimized anode supported cells with a maximum power density of more than 4 A cm$^{-2}$.
- Voltage degradation rate of about 0.1% per 1000 h at 700 °C demonstrated.
- Short stack operated for more than 40,000 h.
- Four 5 kW stacks to be integrated into a 20 kW system showed good reproducibility.

## ARTICLE INFO

## ABSTRACT

The research work of Forschungszentrum Jülich covers many areas ranging from materials development over manufacturing of cells, stack design, mechanical and electrochemical characterization, to systems design and demonstration, always supported by feedback from post-test characterization.

Optimized anode supported cells with two different cathode materials have been standardized with a maximum power density of more than 4 A cm$^{-2}$ (extrapolated) at 800 °C and 0.7 V with hydrogen/air. The use of improved steels, cathodes, contact and protective layers as well as optimized materials processing have resulted in a significant reduction of the voltage degradation rate to about 0.1% per 1000 h at 700 °C demonstrated in an ongoing test for a short stack, which has reached more than 15,000 h of operation. In addition, the benchmark stack of the Real SOFC project has concluded 40,000 h at the beginning of March 2012, and is still in operation.

This behavior has to be verified for larger stacks with cells of a size of 20 × 20 cm$^2$ with most emphasis on design optimization and reduced internal thermo-mechanical stress to ensure gas tight operation. This was shown for four 5 kW stacks to be integrated into a 20 kW system.

## 1. Introduction

Since about 20 years, the SOFC group at Forschungszentrum Jülich has manufactured and operated more than 450 SOFC stacks with power outputs between 100 W and 15 kW. The group has successfully covered topics ranging from materials development and the associated processing technologies over stack design, manufacturing of cells, stacks and components, mechanical and electrochemical characterization and modeling, up to system design and demonstration [1].

* Corresponding author. Tel.: +49 2461 61 6709; fax: +49 2461 61 6695.
E-mail addresses: l.blum@fz-juelich.de (L. Blum), l.g.j.de.haart@fz-juelich.de (L.G.J. (Bert) de Haart), j.malzbender@fz-juelich.de (J. Malzbender), n.h.menzler@fz-juelich.de (N.H. Menzler), j.remmel@fz-juelich.de (J. Remmel), R.SteinbergerWilckens@bham.ac.uk (R. Steinberger-Wilckens).

Two design paths are implemented: light-weight SOFC stacks, which are being developed in the so-called 'cassette design' line for APU (auxiliary power units) applications on trucks, building machines, etc. together with ElringKlinger, Eberspächer and Behr. These designs are required to deliver a short start-up time, robust thermal cycling and operate with diesel reformate. The light-weight stacks potentially reach lifetimes of up to around 10,000 h and are limited by the corrosion resistance of the thin interconnect sheets [2]. The second design (so-called F-Design), on which the article focuses, is less optimized for weight and amount of interconnect material but trimmed to offer a long service time and can be used as a basis for larger stacks. Note, for stationary applications weight plays only a minor role (apart from being reflected in increased materials costs), but long lifetimes of the system and especially the stack are vital.

Jülich work currently concentrates on four areas:

- Improving cell manufacturing and performance at temperatures below 700 °C.
- Further clarifying and predicting degradation phenomena.
- Extending stack lifetime.
- Increasing the robustness of stacks to integrate them in a system's environment.

## 2. Cell development and manufacturing

The development of anode-supported SOFCs at Forschungszentrum Jülich was based on a step-wise optimization of various parameters. In particular, the R&D has been based on the following steps:

1. Developing the base materials and material combinations for the electrolyte (8YSZ), the electrodes (NiO/8YSZ and LSM/8YSZ) and the support (NiO/8YSZ).
2. Manufacturing of first single cells with, to that time, well known technologies like warm pressing (support), vacuum slip casting (anode, electrolyte) and wet powder spraying (cathode, current collector).
3. Scale-up from single cell dimensions $5 \times 5$ cm$^2$ to stack cell sizes of $10 \times 10$ cm$^2$ and $20 \times 20$ cm$^2$.
4. Optimization of layer microstructures, thicknesses and chemical compositions (e.g. ratio LSM/8YSZ within the cathode) [3] and anode thickness [4].
5. Development of novel high power density cathode materials like mixed ionic-electronic conducting LSCF (lanthanum strontium cobalt ferrite) [5,6] and, in parallel, development of thin film processes for special layers like the CGO (gadolinia doped ceria) diffusion barrier (physical vapor deposition, sputtering) [7].
6. Shifting from the classical manufacturing technologies to tape casting for the support and screen printing of all functional layers to adapt the manufacturing line to industrial necessities.
7. Reduction of support thickness from 1.0 to 1.5 mm thick supports to thinner tape-cast supports (0.5 mm) [8].
8. Introduction of wet chemical thin film techniques, e.g. for the electrolyte (sol−gel techniques) [9,30].

Based on these developments current "standard" anode-supported SOFCs from Jülich are:

- For power stacks ($20 \times 20$ cm$^2$ cells) still thick supports, manufactured by warm pressing, with all layers screen printed.
- For short stacks and single cells, a tape-cast support with screen printed layers.
- In all cases a screen printed diffusion barrier layer made of CGO is applied when an LSCF cathode is used (for an operating temperature of 700 °C).

Electrochemical characterization yields the following data:

- At 800 °C and 0.7 V (H$_2$/3%H$_2$O, air) single cells with LSM (lanthanum strontium manganese)-type cathode deliver 1.5 A cm$^{-2}$ [29] and single cells with LSCF cathode and screen printed CGO layer deliver 1.7 A cm$^{-2}$ [4].
- With sputtered or PVD (physical vapor deposition) CGO layer the current density reaches 2.4 A cm$^{-2}$ [7]
- By introducing a thin film 8YSZ electrolyte (1 μm instead of 10 μm), the extrapolated current density is in the range of 4 A cm$^{-2}$, with LSC (lanthanum strontium cobaltite) cathode) [9].
- In the stack environment the LSM based cells deliver around 1.0 A cm$^{-2}$ and the LSCF cathode based cells reach 1.4 A cm$^{-2}$ at 800 °C and 0.7 V.

In the last two years cell development was focused onto the field of cost reduction by way of reducing layer thicknesses, improving the co-firing process of the half-cell and reducing the amount of manufacturing steps. The latest development is a 'fully tape-cast half-cell', starting with casting the electrolyte, afterward followed by casting of the functional anode and subsequently the support green-in-green and finally co-firing the tri-layer system (sequential tape casting). By carefully choosing the raw materials the still used flattening step might also by omitted. Depending on the chosen stack design, the cells (proven up to now to sizes of $10 \times 10$ cm$^2$) can be cut in green state and sintered to near-net-shape. The maximum deviation in length and width is in the range of 1%, e.g. for $10 \times 10$ cm$^2$ squared cells this amounts to ±0.5 mm [10].

Fig. 1 gives an overview of the cell development in the last 17 years and mentions some of the most important R&D results. Fig. 2 illustrates the state-of-the-art of the cell manufacturing route for $10 \times 10$ cm$^2$ cells.
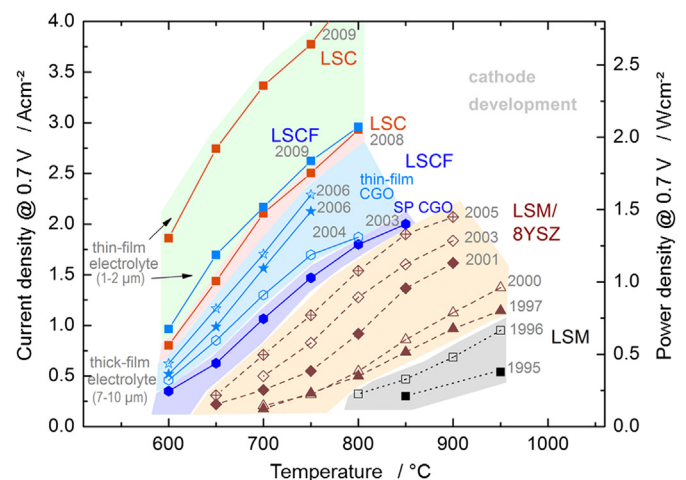


**Fig. 1.** Current density as function of operating temperature for single cell tests in ceramic housing (H$_2$/H$_2$O, air, low fuel utilization) from 1995 to 2009.
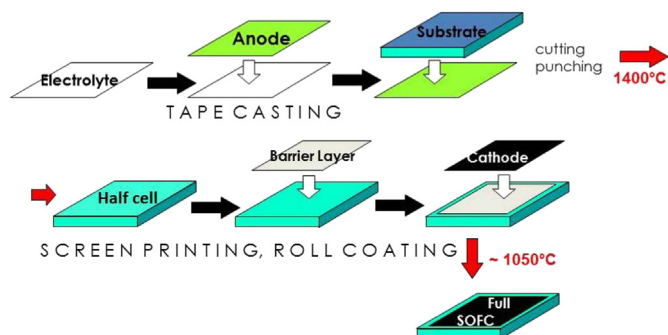
**Fig. 2.** Manufacturing scheme of current anode-supported SOFCs at Forschungszentrum Jülich.

## 3. Degradation mechanism by Cr-poisoning

Intensive research activities of single cells and cells in real stacks yielded experimental evidence for the mechanisms of the poisoning of $(La,Sr)MnO_3$ (LSM) cathodes by volatile chromium species which are formed through evaporation from the chromium containing oxide layers of the steel interconnectors in SOFC stacks. Then the chromium compounds either are reduced at the three-phase boundary electrolyte/cathode/gas phase or they interact with the material of the cathode.

Based on electrochemical measurements with cells with LSM cathodes with and without the presence of a chromium source and applying wet chemical and scanning electron microscope post-test analysis methods, the resulting effects of the volatile chromium species on the LSM cathodes could be explained.

The chromium source was realized in equivalence to current stack technologies by using the ferritic high chromium steel Crofer22APU, either with bare surface or of which the surface was modified by adding first $Mn_3O_4$ as protective layer and in a subsequent step a perovskite powder (Jülich type LCC10) as cathode contact layer.

The time dependent degradation of cells exposed to a chromium source during assembly and operation under load can be divided into three phases: a conditioning phase, a phase with weak linear degradation and a phase with strong but still rather linear degradation. The use of different coatings clearly reduces the degradation rate (see Fig. 3) by virtue of a reduced chromium release.

Based on the investigations carried out, three reaction mechanisms of chromium species could be identified for LSM cathodes [11,12]:

1. Gaseous chromium species form a chromium-manganese-spinel within the current collector layer by interacting with manganese oxide phases. This interaction is the origin of the main part of chromium content in the cathode, but it does not result in measurable degradation.
2. Gaseous chromium species adsorb at the surface of LSM and inhibit the oxygen adsorption and diffusion toward the electrochemical active zone. This increases the activation polarization of the cathode but does not cause significant chromium deposition (phase I in Fig. 3)
3. Gaseous chromium species are reduced in the electrochemically active zone and form $Cr_2O_3$. In the long term this causes an accumulation of chromium in the cathode, which fills up pores (phase II in Fig. 3). By the interaction of $Cr_2O_3$ with LSM a chromium-manganese-spinel is formed. The continuous extraction of manganese from the LSM leads to a change of the stoichiometry of the perovskite until the stability limit is reached. From that point on a stepwise decomposition starts. This decomposition affects the microstructure of the cathode as well as the conductivity of the LSM matrix and marks the beginning of strong degradation (phase III in Fig. 3). In case of applying a chromium evaporation protection layer ($Mn_3O_4$) and a cathodic contacting layer (LCC10) which acts additionally as Cr getter the cells do not fall into phase III degradation within the experimental time frame of 3500 h. As can be seen from the long term test of more than 40,000 h with the short stack presented in Fig. 8, also for such a long operation time phase III does not occur.

## 4. Stack development

One of the main focal points of the development work in Jülich is the realization of robust large stacks, incorporating $20 \times 20$ cm$^2$ sized cells. Already in 2004 it was demonstrated that it is possible to manufacture and assemble these type of stacks and operate them in a furnace by testing a 60 layer F′20-stack with methane/steam (internal reforming) delivering a power output of almost 12 kW [13].

Based on the F20-design, described in Ref. [14], some modifications were implemented during recent years to deal with several potentially unfavorable or harmful issues that might arise during various operation modes. First of all the manifold dimensions had to be enlarged to guarantee a uniform gas flow distribution to all single layers (F′20-design). For the case of a 36-layer stack in counter flow (basic configuration for 5 kW stack power) the result of a CFD-calculation is shown in Fig. 4. The deviation from the mean volume flow on the fuel side is less than ±2%, which is clearly below the target of ±5%.
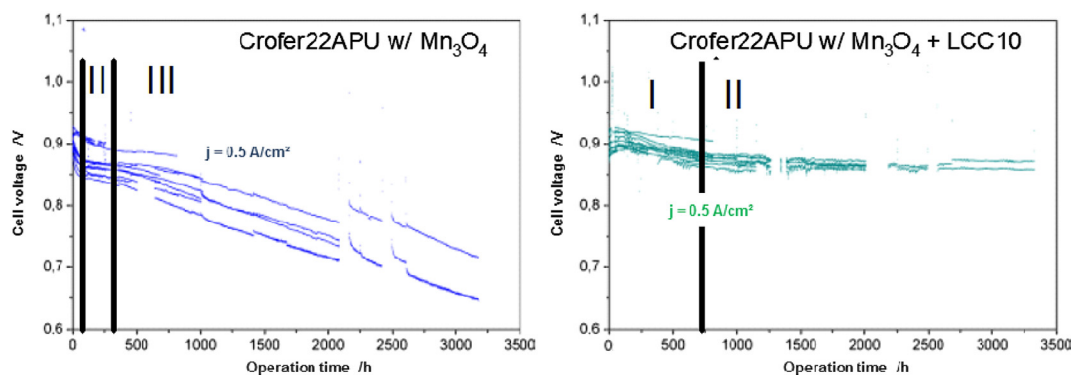


**Fig. 3.** Degradation of single cells with LSM cathode in presence of a chromium source on the air side. Left: Crofer22APU with protective layer $Mn_3O_4$. Right: Crofer22APU with protective layer $Mn_3O_4$ and contact layer LCC10. Areas of strong (I), weak (II), and again strong (III) voltage degradation as function of time and of coating are indicated.
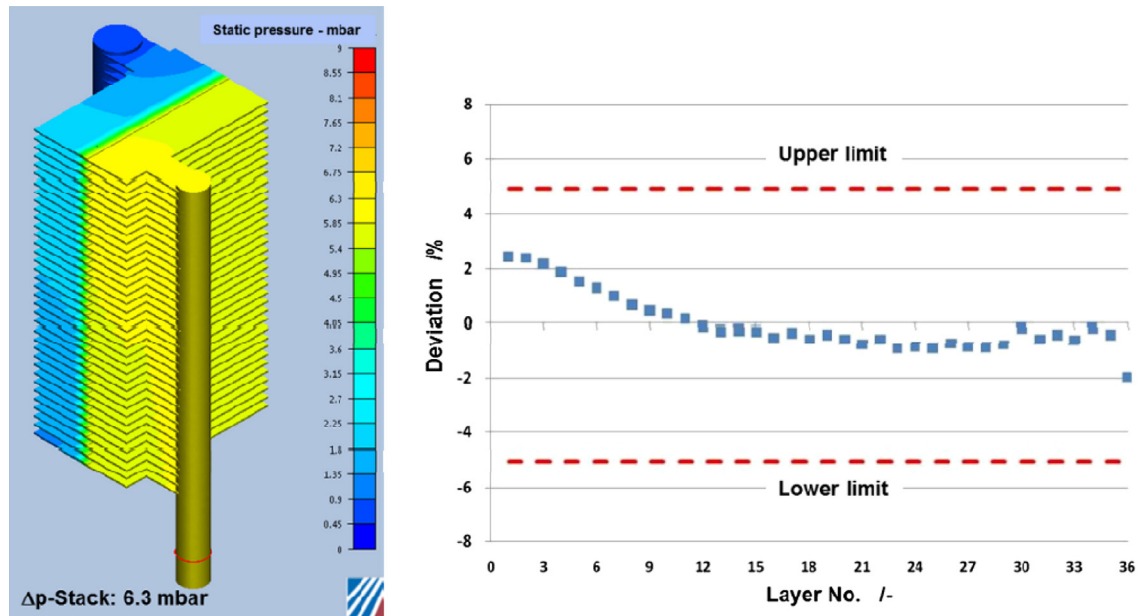
**Fig. 4.** Flow distribution on the fuel side of a 36 layer stack (F'2036).

The other source of failure is thermo-mechanical stress acting on the various components of the stack; especially the glass ceramic used for sealing the metal parts to each other and the cell to the interconnect was of concern here. Thermo-mechanical analyses based on modeling and experimental analysis are currently major central efforts in Jülich in order to find solutions to accommodate the forces that are raised, to reduce the associated stresses and/or to develop sealing materials and concepts that allow accommodating higher mechanical stress. Initial tests revealed that a massive problem can be caused by bending associated instabilities of thin parts of the metallic plates in the manifold area and by the positioning rods placed in boreholes, which were used in the past to assure a strict parallel settling of the single plates with respect to each other. As illustrated in Fig. 5, various new design variants take this into account by using short rods that guide only one layer with respect to the next and additionally re-enforcing points in the thin manifold parts are added (F''20-design). Guiding rods positioned outside the plates are another option (F$^A$20-design). Enlarged area for the sealing glass to improve the bonding and round manifold channels to reduce the thermomechanical stress have been the next step in design improvement (F'''20-design).

With the aid of finite element modeling a better understanding of the phenomena was attained and, in combination with improved sealing material, promising results could be achieved, as described in Ref. [15]. However, thermo-mechanical aspects remain critical. For example small deviations in dimensions can still cause problems with the guiding system. Therefore an optimized stack assembly was tested without guiding rods (F'''*20-design) which showed very promising initial results. Following this route four stacks with 36 layers each showed leakage rates from fuel side to air side within the stack and to the environment of more than one order of magnitude below the required limit. This limit is set at 1% of the fuel flow entering the stack in case of methane operation (completely reformed with a steam to carbon ratio (S/C) of 2.2) with 70% fuel utilization at 0.5 A cm$^{-2}$ and with a pressure difference between inner anode and air compartments and to the environment of 100 mbar. This result is much better than those of the previous stacks (see Fig. 6). The leakage rates are determined at
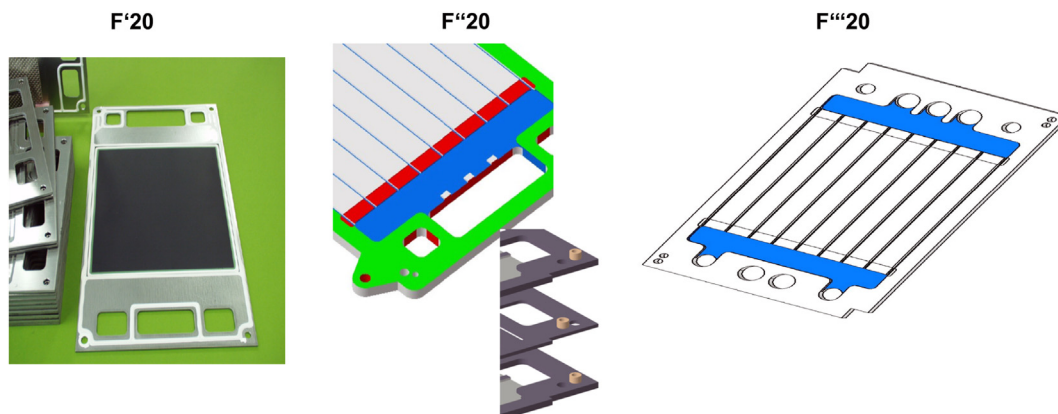


**Fig. 5.** F20-design development steps (the different colors only help visualizing the different depths in the plate) (For interpretation of the references to color in this figure legend, the reader is referred to the web version of this article.).
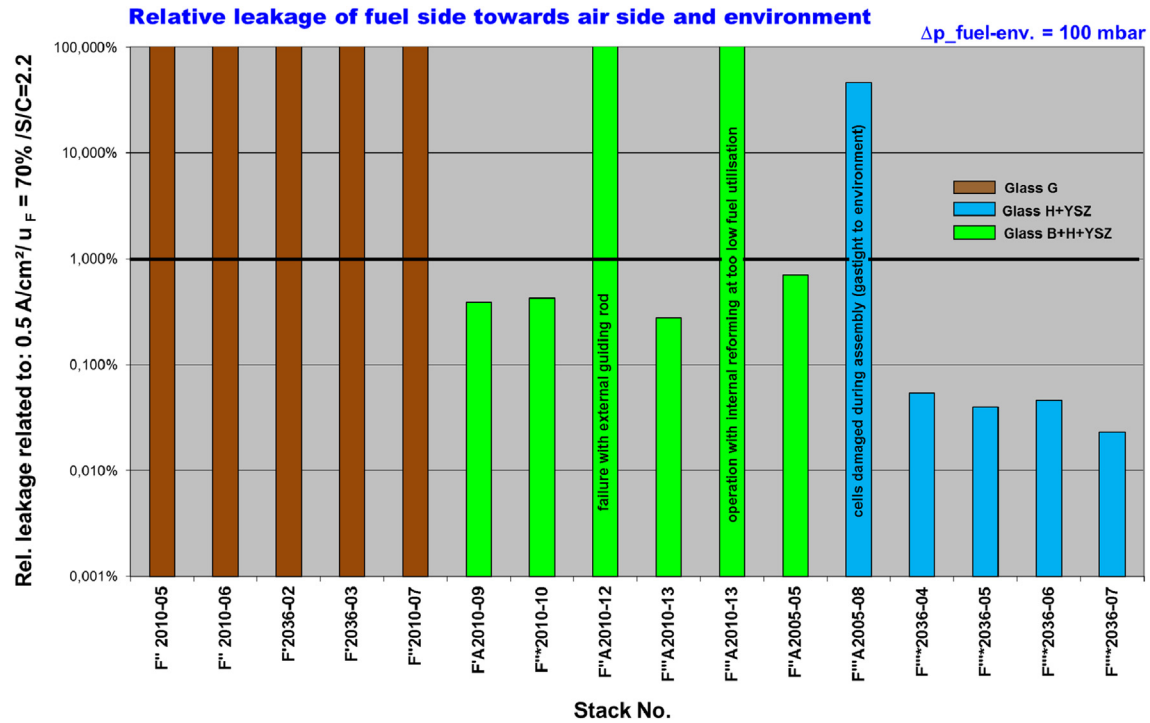
**Fig. 6.** Relative leakage of various stacks from fuel side to air compartments and to the environment in case of 100 mbar pressure difference.

room temperature by applying a certain gauge pressure on fuel side, on air side and simultaneously on both sides and measuring the pressure drop as function of time.

The fact that not only design issues are essential is revealed by the test of stack F‴2010-13 (see Fig. 6). After a first operation with hydrogen the stack was cooled down and leak tested. The result was very promising. However, after a second test phase with methane/steam (internal reforming) the leak rate increased by three orders of magnitude. The reason for this leakage can be explained by the temperature profile of the stack depicted in Fig. 7. The profile was measured with thermocouples placed in the interconnect plate in the middle of the stack. The furnace temperature was 800 °C.

Operating the stack with methane with a relatively low fuel utilization of 40% causes a large temperature gradient in the manifold (green line in Fig. 7) which results in fatally high stresses in the glass ceramic sealing, as calculated in Ref. [15]. In case of fuel utilization values of 70% or higher (brown line in Fig. 7), which is required in a system, the temperature differences in the manifold are similar to hydrogen operation (red line in Fig. 7). Both should not result in an increased leakage, which corresponds to the leakage measured after the first operation phase. A comparison of the behavior of stacks operated in a furnace and stacks operated in a thermal insulation in a system is currently investigated with FEM. First results of stack modeling are described in Ref. [16].
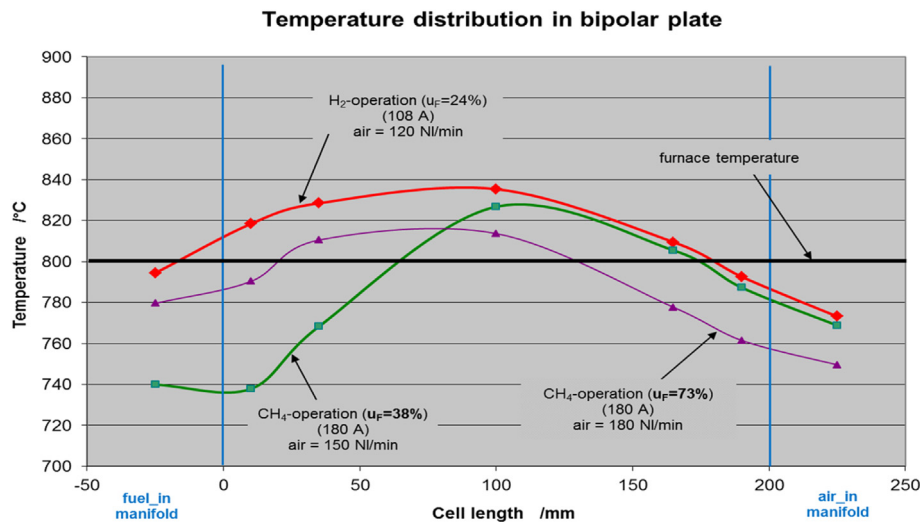


**Fig. 7.** Stack F‴A2010-13: Measured temperature distribution in the stack from fuel in to fuel out (=air in) in case of different fuel gases and fuel utilization $u_F$ (measured points connected via a polynomial curve).
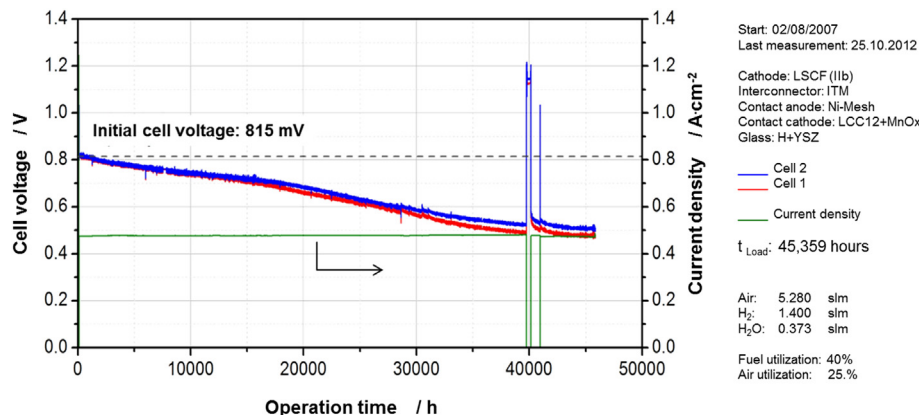
**Fig. 8.** Cell voltages as function of operating time for stack F1002-97 (slm − standard liters per minute).

## 5. Stack testing

Consequences from all these findings will be implemented in the design of the next stack generation which is currently under preparation.

Stack testing in Jülich is generally performed with respect to two aspects. One is to investigate the performance and durability using various material combinations. This is done with short stacks with 2–5 layers (cells 10 × 10 cm², effective electrode area 80 cm²). The second aspect is to investigate the behavior of larger stacks, with an increased number of layers (from 10 up to 60) as well as an increased effective electrode area of 360 cm² (cells 20 × 20 cm²). These larger stacks incorporate design changes based on test results and on modeling.

Based on the work initiated by the EU Integrated Project Real-SOFC [17] the long term behavior has been tested in various short stacks in dependence of operating conditions. In fact, the stack F1002-97 is under operation since August 2007 at a furnace temperature of 700 °C under a load of 500 mA cm⁻² and humidified hydrogen (20% humidity) at a fuel utilization of 40% and dry compressed air with 25% oxygen utilization. Representing the

development status of 2007, the cathode is LSCF with a screen-printed CGO diffusion barrier and with a perovskite contact layer (LCC12). An additional protective manganese oxide layer ($MnO_x$) was applied on the metal interconnects which in this case were manufactured from the ITM material of Plansee [18]. Both layers are applied by wet powder spraying (WPS) and will not completely retain the chromium release from the metal plate. The stack has now achieved more than 45,000 h of operation under load, which is the longest time reported so far for a stack with planar anode supported cells. The average voltage loss is 7.5 mV per 1000 h, which corresponds to a relative voltage degradation of 0.9% per 1000 h. The voltage time plot is shown in Fig. 8.

An improved retention of chromium is expected, if a protective layer is applied by atmospheric plasma spraying (APS) because of its distinctive higher gas tightness of approx. 95% compared to about 80% in case of a WPS layer. In the stack F1004-21 such a 40 μm thick layer (MnCoFe-oxide (MCF) on Crofer22APU) is currently tested under the same conditions as in the case of stack F1002-97. Stack F1004-21 shows extremely good current–voltage characteristics, due to the combination of the LSCF cathode with the CGO diffusion barrier applied by PVD: all four layers yield 1.2 A cm⁻²@0.7 V @700 °C (see Fig. 9). Until now, the stack has been operated for
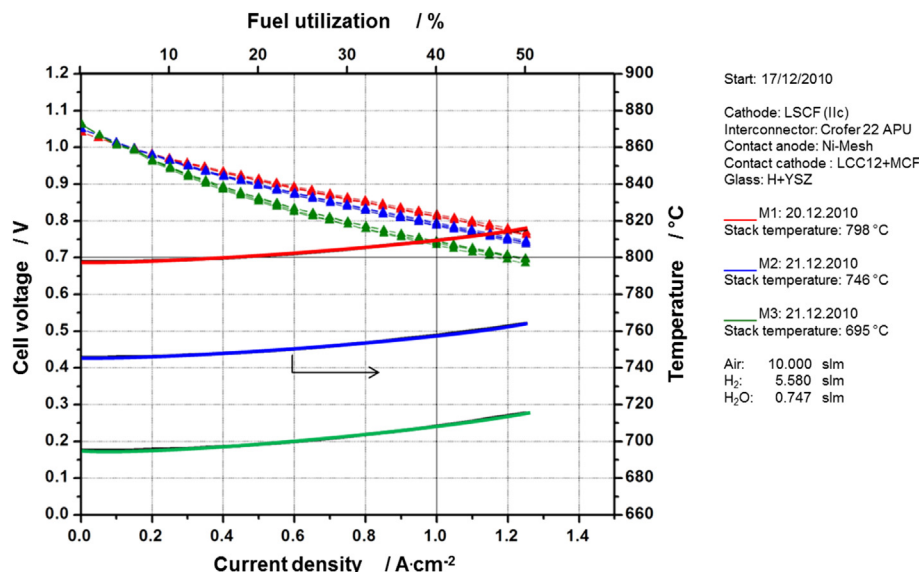


**Fig. 9.** Current−voltage characteristics of stack F1004-21 at various temperatures.

more than 15,000 h, showing an average voltage loss of 1 mV per 1000 h, which corresponds to a relative voltage degradation of 0.12% per 1000 h. The voltage time plot is shown in Fig. 10.

Stacks with larger cells of $20 \times 20$ cm$^2$ outer dimensions with an effective electrode area of 360 cm$^2$ have been used in tests since the year 2000. After the demonstration of a first 1 kW stack at the end of 2000, followed by stacks with 9.2 kW in 2002 [19] and with 13.3 kW in 2004 [13], the main focus was on the improvement of the stack thermo-mechanical robustness. A key issue is the transfer of the sealed and reduced stack from the furnace to the system, which leads to different and more pronounced requirements onto the thermo-mechanical stability of the stack. As described in Ref. [15] a large number of investigations and improvements (design, operation conditions, materials, quality assurance) have been necessary to reach a status where the transfer of a stack into a system is possible. A first demonstration of stack operation outside the furnace was done in a project using coal mine gas as a fuel [20]. With the additional improvements as described above, also the four 5 kW stacks to be integrated into a 20 kW system [21] showed the required performance and sufficient gas tightness. Necessary optimization of the system components for the 20 kW system like air pre-heater and pre-reformer by CFD and FEM is described in Refs. [22,23].

Fig. 11 shows the current–voltage characteristics of the four 5 kW stacks measured in a furnace at 700 °C. The curves are nearly identical; the stacks yielding between 7.3 and 7.5 kW at 0.7 A cm$^{-2}$ at average cell voltages between 800 and 830 mV.

The deviation of cell voltages within one stack at maximum load (0.7 A cm$^{-2}$) is shown in Fig. 12. The distribution is very uniform except for the layers at bottom and top of the stack. This is mainly an effect of the local temperature, which is always slightly lower at these positions. Only layer 5 of stack F‴2036-04 reveals a larger deviation, which is most likely caused by contacting problems.

## 6. Post test analysis

After operation, stacks are regularly dismantled to analyze the degradation and failure mechanisms. Obviously, in a stringent post mortem methodology, advanced characterization methods are an essential element to understand the stack performance within the frame-work of systematic testing [24].

Disassembling is carried out with selected experts depending on expected outcome of the post-operational analysis and/or the goals set in initiating the stack experiment. Experts are available from synthesis, production, and interaction of materials, thermo-mechanics, corrosion, thermo-chemistry, sealants, stack/system
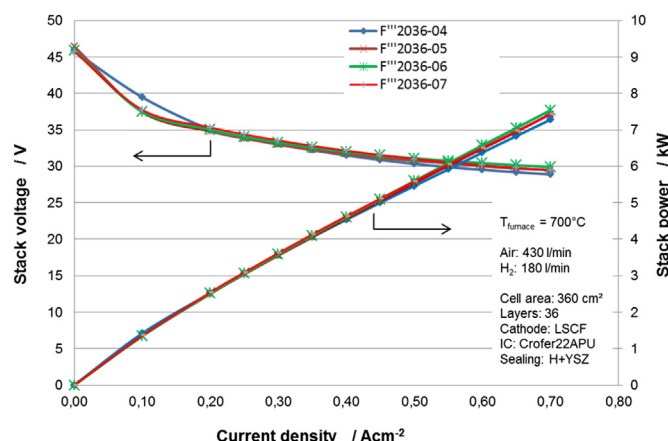


**Fig. 11.** Current–voltage characteristics of four 5 kW stacks.

operation, single cell testing, optical and scanning electron microscopy. As an indication of the amount of analyses performed in this area, it should be noted that around 150 dissections were carried out in the time from August 2002 to May 2012.

During the post operational analysis, electro-chemical results and irregular events receive special attention and cells and components that display unusual operational behavior are inspected in detail. A digital photographic image is taken of every stack plane during disassembly. Unusual observations are investigated microscopically. After dismantling, more detailed SEM (TEM) investigations are carried out as necessary. Investigation methods cover graphical and image analysis to gain insight into macroscopic changes and associated shifts in color. SEM and EDX deliver information on microscopic/structural changes, in order to acquire a qualitative chemical analysis. Furthermore, wet chemical analysis is used in a coarsely localized quantitative analysis. Thermography and computer tomography have shown to be successful in determination of the origins of short circuits and localization of porosities. XRD offers insight into structural changes, TEM into local changes in interfaces and reactions. Leakages are localized using liquid dyes.

A topic that has been specifically addressed in connection with the long-term testing is the profound understanding of degradation phenomena under steady state operation. Chromium poisoning is believed to be one influential parameter and has received significant attention in Jülich in the past years [25,26]. The work of the post operational analysis group has helped to understand and
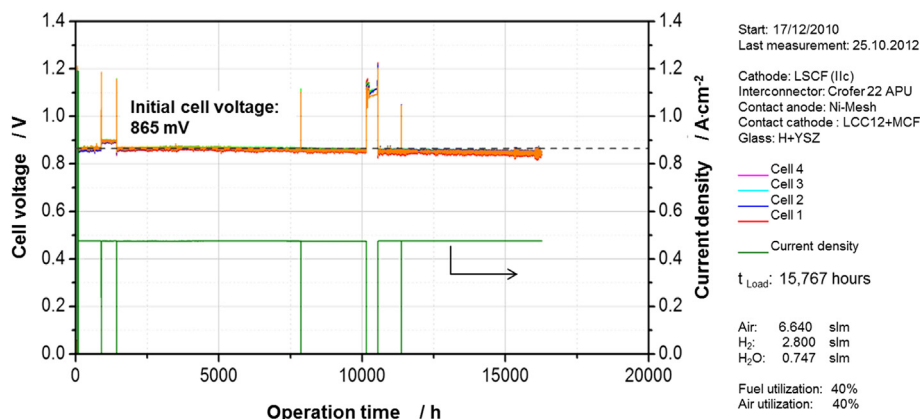


**Fig. 10.** Cell voltages as function of operation time for stack F1004-21.
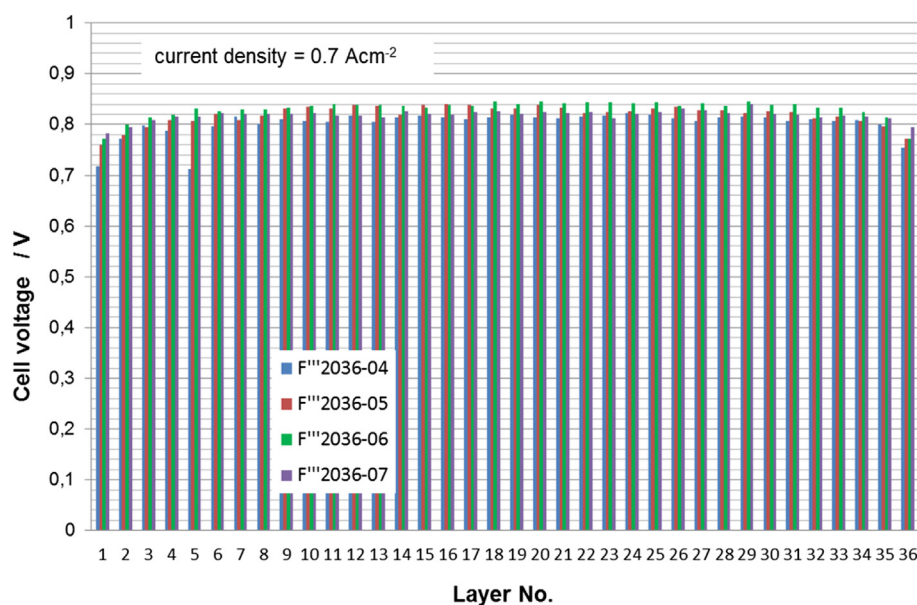
**Fig. 12.** Cell voltages of four 5 kW stacks with 36 layers at 0.7 A cm$^{-2}$ and 700 °C.

improve the stack design and long term stability by highlighting other potential reaction and degradation sources, for example sealant-steel and cathode reactions, re-oxidation and localized creep associated deformations [27].

Within the framework of post-test investigation on the degradation phenomena of long term operated stacks detailed analyses have been carried out for stacks operated 17,000 h at 700 °C with an average degradation rate of 10 mV per 1000 h at 500 mA cm$^{-2}$ [27] and about 19,000 h at 800 °C (with additional protective layer) with 4 mV per 1000 h at 500 mA cm$^{-2}$ [28].

In addition to the differences in operation temperature it should be noted that the stack operated at 700 °C had an LSCF cathode with CGO diffusion barrier and a protective slurry coating and the one operated at 800 °C had an LSM cathode and an atmospheric plasma sprayed coating. Whilst the stack operated at 700 °C was shut down after progressive degradation, the stack operated at 800 °C was shut down after failure of one cell.

In summary, the parts of the stack operated at 700 °C showed only small changes and interactions, including the anode [27]. The cell microstructure appeared to be slightly modified. Two findings may play a role with respect to long-term stack stability. Firstly, local dot-like iron oxide formation may cause eventually short circuiting, if the oxide bridges the sealing gap after even longer operating times. Furthermore, it was suggested that the progressive degradation might be a result of strontium chromate formation.

For the stack operated at 800 °C no significant Cr contents could be found in the cathode thus verifying that the MCF layer applied by APS is an efficient Cr barrier which can reduce the formation of strontium chromate or of chromium manganese spinels at the cathode/electrolyte interface [28]. However, Mn diffusion into 8YSZ led to local accumulation at the grain boundaries which probably caused a decrease in conductivity and a mechanical weakening and eventual micro-cracking at the grain boundaries followed by continuing crack growth. The growth of these cracks eventually resulted in the fracture of one cell, burning of fuel gas and sudden failure of the stack.

From the results of both stacks, it can be concluded that the targeted operation times of SOFC stacks can become realistic by combining an LSCF cathode with an APS protective coating, which is realized in a currently ongoing stack test.

Because all stack tests have been performed with pure hydrogen (gas purity better than 99.9%) nothing can be said about the effect of impurities supplied with the gases, especially sulfur compounds. Up to now work concentrated on the stack components inherent interactions. Effects coming from outside the stack will be investigated in the next phase.

## 7. Summary and outlook

The results of the work performed in Jülich so far, reveal, that a tremendous progress has been achieved in the recent years. Cell manufacturing has advanced toward low cost technologies and at the same time the potential of extremely high power densities could be shown. Long term stability has improved in a way that in a test lasting more than 15,000 h, a degradation rate below the target for stationary operation is achieved. A short stack has been operated for more than 45,000 h without catastrophic incidents, which shows, that there is no fundamental effect preventing such a long term operation of SOFC with metallic interconnectors. The challenge of operating larger stacks in a real environment is being tackled and first promising results with robust stacks have been achieved. The next steps will be to integrate all the findings in the next generation of stack design and to show the reliable operation of stacks in a system.

## References

[1] R. Steinberger-Wilckens, L. Blum, H.P. Buchkremer, S.M. Gross, L.G.J. de Haart, K. Hilpert, H. Nabielek, W.J. Quadakkers, U. Reisgen, R.W. Steinbrech, F. Tietz, Int. J. Appl. Ceram. Technol. 3 (6) (2006) 470—476.
[2] P. Huczkowski, W.J. Quadakkers, Effect of geometry and composition of Cr steels on oxide scale properties relevant for interconnector applications in

solid oxide fuel Cells (SOFCs), in: Schriften des Forschungszentrums Jülich, Reihe Energietechnik/Energy Technology, 65, Forschungszentrum Jülich, 2007.

[3] V.A.C. Haanappel, J. Mertens, D. Rutenbeck, C. Tropartz, W. Herzhof, D. Sebold, F. Tietz, J. Power Sources 141 (2) (2005) 216—226.

[4] N.H. Menzler, V.A.C. Haanappel, J. Power Sources 195 (2010) 5340—5343.

[5] A. Mai, V.A.C. Haanappel, S. Uhlenbruck, F. Tietz, D. Stöver, Solid State Ionics 176 (2005) 1341—1350.

[6] A. Mai, V.A.C. Haanappel, F. Tietz, D. Stöver, Solid State Ionics 177 (2006) 2103—2107.

[7] S. Uhlenbruck, N. Jordan, D. Sebold, H.P. Buchkremer, V.A.C. Haanappel, D. Stöver, Thin Solid Films 515 (2007) 4053—4060.

[8] W. Schafbauer, Entwicklung und Herstellung von foliengegossenen, anodengestützten Festoxidbrennstoffzellen, Dissertation, in: Schriften des Forschungszentrums Jülich, Band 66, Ruhr-Universität Bochum, 2009, ISBN 978-3-89336-631-6.

[9] F. Han, R. Mücke, T. van Gestel, A. Leonide, N.H. Menzler, H.P. Buchkremer, D. Stöver, J. Power Sources 218 (2012) 157—162.

[10] N.H. Menzler, W. Schafbauer, W. Deibert, R. Kauert, H.P. Buchkremer, Kostengünstiges Herstellungsverfahren für anodengestützte Festoxid-Brennstoffzellen (SOFC), in: Presentation at the Annual Meeting of the German Ceramic Society (DKG), March 5—7 2012, Nuremberg, Germany, 2012.

[11] A. Neumann, Chrom-bezogene Degradation von Festoxid-Brennstoffzellen, Dissertation, in: Schriften des Forschungszentrums Jülich, Reihe Energie & Umwelt, Band 98, Ruhr-Universität Bochum, 2010.

[12] M. Kornely, A. Neumann, N.H. Menzler, A. Leonide, A. Weber, E. Ivers Tiffée, J. Power Sources 196 (17) (2011) 7203—7208.

[13] L. Blum, H.P. Buchkremer, S.M. Gross, L.G.J. de Haart, W.J. Quadakkers, U. Reisgen, R. Steinberger-Wilckens, R.W. Steinbrech, F. Tietz, Overview of the development of solid oxide fuel cells at Forschungszentrum Jülich, in: Proc. of the Electrochemical Society (SOFC IX), 2005, pp. 39—47.

[14] R. Steinberger-Wilckens, I.C. Vinke, L. Blum, J. Remmel, F. Tietz, W.J. Quadakkers, Progress in SOFC stack development at Forschungszentrum Jülich, in: Proc. of the 6th European SOFC Forum, Luzern/CH, 2004, pp. 11—19.

[15] L. Blum, S.M. Groß, J. Malzbender, U. Pabst, M. Peksen, R. Peters, I.C. Vinke, J. Power Sources 196 (2011) 7175—7181.

[16] M. Peksen, Int. J. Hydrogen Energy 36 (18) (2011) 11914—11928.

[17] L.G.J. de Haart, J. Mougin, O. Posdziech, J. Kiviaho, N.H. Menzler, Stack degradation in dependence of operation parameters: the real-SOFC sensitivity analysis, in: Proc. of the 8th European Solid Oxide Fuel Cell Forum, Lucerne/CH, 2008. Paper No. B1002.

[18] A. Venskutonis, G. Kunschert, et al., in: Proc. of the 8th European Solid Oxide Fuel Cell Forum, Lucerne/CH (2008). Paper No. A0906.

[19] L. Blum, L.G.J. de Haart, I.C. Vinke, D. Stolten, H.P. Buchkremer, F. Tietz, G. Blaß, D. Stöver, J. Remmel, A. Cramer, R. Sievering, Planar anode substrate type SOFC kW-class stack development, in: Proc. of the 5th European Solid Oxide Fuel Cell Forum, Lucerne/CH, 2002, pp. 784—790.

[20] B. Groß, L. Blum, L.G.J. de Haart, A. Dengel, J. Power Sources 196 (12) (2011) 5309—5316.

[21] L. Blum, R. Peters, P. David, S.F. Au, R. Deja, W. Tiedemann, Integrated stack module development for a 20 kW system, in: Proc. of the 6th European Solid Oxide Fuel Cell Forum, Luzern/CH, 2004, pp. 173—182.

[22] M. Peksen, R. Peters, L. Blum, D. Stolten, Int. J. Hydrogen Energy 36 (7) (2011) 4400—4408.

[23] M. Peksen, R. Peters, L. Blum, D. Stolten, Int. J. Hydrogen Energy 36 (11) (2011) 6851—6861.

[24] J. Malzbender, R.W. Steinbrech, J. Power Sources 173 (2007) 60—67.

[25] M. Kornely, A. Neumann, N.H. Menzler, et al., ECS Trans. 35 (1) (2011) 2009—2017.

[26] N.H. Menzler, P. Batfalsky, L. Blum, Studies of material interaction after long-term stack operation, in: Proc. of the 7th European Solid Oxide Fuel Cell Forum, Luzern/CH, 2007, pp. 356—363.

[27] N.H. Menzler, P. Batfalsky, S.M. Gross, V. Shemet, F. Tietz, ECS Trans. 35 (1) (2011) 195—206.

[28] J. Malzbender, P. Batfalsky, R. Vaßen, V. Shemet, F. Tietz, J. Power Sources 201 (2011) 196—203.

[29] V.A.C. Haanappel, N. Jordan, A. Mai, J. Mertens, J.M. Serra, F. Tietz, S. Uhlenbruck, I.C. Vinke, M.J. Smith, L.G.J. de Haart, J. Fuel Cell Sci. Technol. 6 (2009) 021302.

[30] F. Han, Sol—gel and Nano-suspension Electrolyte Layers for High-performance Solid Oxide Fuel Cells. PhD Thesis, in: Schriften des Forschungszentrums Jülich, Reihe Energie & Umwelt, Vol. 100, Ruhr University Bochum, 2010, ISBN 978-3-89336-694-1.